

A Practical Performance Evaluation Method for Electric Multicopters

Dongjie Shi, Xunhua Dai, Xiaowei Zhang, and Quan Quan

Abstract—Multicopters are attracting more and more attention these years. In the design stage, designers and users wonder if an assembled multicopter can meet their performance requirements, such as hovering endurance, system efficiency, maximum load, maximum pitch, and maximum flight distance. However, in practice, they used to evaluate the performance of a multicopter through lots of flight experiments or by experience, which are normally inefficient and costly. This motivates us to propose a comprehensive offline evaluation algorithm of multicopter performance. The performance indices considered are mainly determined by the propulsion system, including motors, propellers, electronic speed controllers, and batteries. Therefore, in the first stage of this research, models are established for the components of a propulsion system. In order to facilitate the application, only technical specifications of components offered by manufacturers are required as the input of the models. Based on the models and their relationships, equations describing performance indices are established and then solved to perform the evaluation. Finally, several examples are given to demonstrate the efficiency of the proposed evaluation method. As a result, a website (www.flyeval.com) is established, which can provide users with the performance evaluation mentioned in this paper.

Index Terms—Modeling, multicopters, performance evaluation, propulsion systems, quadcopters.

NOMENCLATURE

A	Aspect ratio.
B_p	Number of blades.
C_b	Battery capacity (mAh).
C_M	Torque coefficient.
C_T	Thrust coefficient.
C_d	Drag coefficient.
C_{fd}	Zero-lift drag coefficient.
C_l	Lift coefficient.
C_{\min}	Battery minimum capacity (mAh).
c_p	Blade average chord length (m).
D_p	Propeller diameter (m).

E_a	Back-electromotive force (V).
e	Oswald factor.
G	Total weight (N).
G_b	Battery weight (N).
G_e	Electronic speed controller (ESC) weight (N).
G_m	Motor weight (N).
$G_{\max\text{load}}$	Maximum load (N).
G_p	Propeller weight (N).
\hat{H}_p	Propeller geometric pitch (m).
h	Altitude (m).
I_b	Battery current (A).
I_{control}	Flight controller current (A).
I_e	ESC input current (A).
$I_{e\text{Max}}$	Maximum ESC current (A).
I_m	Equivalent motor current (A).
$I_{m\text{Max}}$	Maximum motor current (A).
I_{m0}	Actual motor nominal no-load current (A).
\hat{I}_0	No-load current (A).
K_E	Back-electromotive force constant.
K_T	Torque constant.
K_{V0}	Nominal no-load motor constant (r/min/V).
K_b	Maximum discharge rate (C).
K_0	Slope of lift curve.
L	Propeller lift (N).
M	Propeller torque (N·m).
N	Motor speed (r/min).
N_{m0}	Nominal no-load speed (r/min).
N_0	No-load speed (r/min).
\hat{N}_0	Actual no-load speed (r/min).
n_r	Number of rotors.
P_{Fe}	Iron loss (W).
P_{Fe0}	Nominal iron loss (W).
R_b	Battery resistance (Ω).
R_e	ESC resistance (Ω).
R_m	Motor resistance (Ω).
S_{sa}	Blade area (m ²).
T	Propeller thrust (N).
T_b	Time of endurance (min).
T_e	Electromagnetic torque (N·m).
T_{fly}	Total flight time (min).
T_{loiter}	Hovering endurance (min).
T_t	Environment temperature ($^{\circ}\text{C}$).
T_0	No-load torque (N·m).
U_b	Battery voltage (V).
U_e	ESC input voltage (V).
U_{e0}	Equivalent dc voltage (V).

Manuscript received March 2, 2016; revised August 19, 2016 and December 4, 2016; accepted January 30, 2017. Date of publication March 2, 2017; date of current version June 14, 2017. Recommended by Technical Editor H. Gao. This work was supported by the National Natural Science Foundation of China under Grant 61473012 and Grant 61603014. (Corresponding author: Quan Quan.)

The authors are with the School of Automation Science and Electrical Engineering, Beihang University, Beijing 100191, China (e-mail: qq_buaa@buaa.edu.cn).

Color versions of one or more of the figures in this paper are available online at <http://ieeexplore.ieee.org>.

Digital Object Identifier 10.1109/TMECH.2017.2675913

U_m	Equivalent motor voltage (V).
U_{m0}	Motor nominal no-load voltage (V).
V	Flight speed (m/s).
V_{\max}	Maximum flight speed (m/s).
W	Airspeed of a blade (m/s).
Z	Flight distance (m).
Z_{\max}	Maximum flight distance (m).
α	Angle of attack (rad).
α_0	Zero-lift angle (rad).
α_{ab}	Absolute angle of attack (rad).
ε	Downwash correction factor.
η	System efficiency.
θ	Pitch (rad).
θ_{\max}	Maximum pitch (rad).
θ_p	Blade angle (rad).
ϕ_0	Helix angle (rad).
ρ	Air density (kg/m ³).
ξ	Position coefficient.
λ	Correction coefficient of the blade airfoil area.
δ	Downwash effect correction angle (rad).
σ	ESC duty cycle.

I. INTRODUCTION

DURING recent years, multicopters are very popular for their unique advantages over fixed-wing airplanes and helicopters in many aspects. First, a multicopter has a simple structure and, therefore, is assembled with little effort. Second, since basic movements are decoupled from each other, the remote control of a multicopter is simple. Third, a multicopter is easy to maintain. Due to these salient features, multicopters have been used in many fields [1]–[4].

To design a multicopter, first of all, a designer has to select components in order to meet the performance requirements, e.g., hovering endurance, system efficiency, maximum load, maximum pitch, and maximum flight distance. Multicopter performance is mainly determined by the chosen propulsion systems, which mainly consist of propellers, brushless dc motors, ESCs, and the battery pack. Different selections of components will lead to different flight characteristics. For instance, increasing the capacity of the battery pack may increase the endurance of flight or prevent a multicopter from taking off because of the increased weight. As far as we understand, in practice, many designers used to evaluate the performance of a multicopter through lots of flight experiments or by experience, which are normally inefficient and costly. Moreover, how the choice of components is related to the performance requirements remains an open problem, which is hard to solve by experiments and experience [5], [6].

In order to solve these problems, an offline method of performance evaluation will be proposed in this paper. To the best of the authors' knowledge, few research results exist in terms of the performance evaluation of multicopters. In [7], wind-tunnel experiments were carried out to show the variation of the propeller thrust coefficient, the torque coefficient, and the efficiency caused by different Reynolds numbers. In [8] and [9], the motor modeling is detailed. In [10], experiments were performed to study the effect of controller firmware on

multicopter actuator dynamics. However, in all of these papers, models of the propulsion system are not provided explicitly, let alone performance evaluation. In [11], the thrust coefficient and the torque coefficient are expressed in complicated forms, which are difficult to be directly used in practice. In [12] and [13], both the propeller model and the motor model are given, but there exist a few undetermined parameters in these models, such as the lift coefficient and the torque coefficient, which need to be determined through a lot of experiments. In practice, for a component, manufacturers often only offer several parameters (e.g., for a propeller, the diameter, the pitch, and the blade number are given). However, they are not related directly to the existing models. In [14] and [15], the modeling methods of the battery pack, motors, ESCs, and propellers are introduced, but the ESC models are not provided with great detail and the evaluation indices are incomplete as well. For example, flight distance, maximum load, and maximum pitch are not involved. A website www.ecalc.ch/ provides users with a performance evaluation package of multicopters. It is claimed that the evaluation results are reliable. However, the algorithms used for evaluation are not given. Some important performance indices are not considered, such as maximum flight distance.

In this paper, a practical and comprehensive evaluation method is proposed for multicopters to estimate a series of performance indices. For simplicity, the evaluations are formulated as four problems. For applicability purpose, only technical specifications of components offered by manufacturers are required as the input to the models. Testing examples are finally given to show the effectiveness of the proposed method. Furthermore, a website www.flyeval.com is established, which can provide users with the performance evaluation mentioned in this paper.

II. PROBLEM FORMULATION

There are two major tasks in this paper: propulsion system modeling and performance evaluation. Performance evaluation is based on propulsion system modeling, which is divided into four parts: propeller modeling, motor modeling, ESC modeling, and battery modeling. All inputs to components of a propulsion system are taken from the parameters provided by manufacturers, as shown in [Table I](#).

The outputs from propulsion system modeling are a series of performance indices. For simplicity, they are formulated into the following four problems.

- 1) *Problem 1*: In the hover mode, according to the known parameters, estimate the hovering endurance T_{loiter} , the duty cycle of throttle σ , the ESC input current I_e , the ESC input voltage U_e , the battery current I_b , and the motor speed N .
- 2) *Problem 2*: In the maximum thrust mode,¹ according to the known parameters, estimate the ESC input current I_e , the ESC input voltage U_e , the battery current I_b , the motor speed N , and the system efficiency² η .

¹The maximum thrust case is an extreme case of an multicopter, in which motors are at full throttle state.

²System efficiency is the ratio of the propeller output power and the battery power in full open throttle.

TABLE I
PROPULSION SYSTEM PARAMETERS

Component	Parameters
Propeller	$\Theta_p = \{\text{Diameter } D_p, \text{ Pitch } H_p, \text{ Blade Number } B_p, \text{ Propeller Weight } G_p\}$
Motor	$\Theta_m = \{\text{Nominal No-load Motor Constant } K_{V0}, \text{ Maximum Current } I_{m\text{Max}}, \text{ Nominal No-load Current } I_{m0}, \text{ Nominal No-load Voltage } U_{m0}, \text{ Resistance } R_m, \text{ Motor Weight } G_m\}$
ESC	$\Theta_e = \{\text{Maximum Current } I_{e\text{Max}}, \text{ Resistance } R_e, \text{ ESC Weight } G_e\}$
Battery	$\Theta_b = \{\text{Capacity } C_b, \text{ Resistance } R_b, \text{ Total Voltage } U_b, \text{ Maximum Discharge Rate } K_b, \text{ Battery Weight } G_b\}$

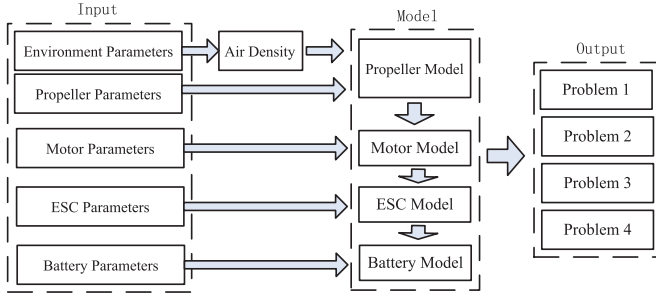


Fig. 1. Modeling procedure.

- 3) *Problem 3*: In the forward flight mode, according to the known parameters, estimate the maximum load G_{maxload} and the maximum pitch θ_{max} , both of which are used to guarantee the safety of a multicopter.
- 4) *Problem 4*: In the forward flight mode, according to the known parameters, estimate the maximum flight speed V_{max} and the maximum flight distance Z_{max} .

The frame of this research is shown in Fig. 1.

III. PROPULSION SYSTEM MODELING

In the section, models for the propeller, the motor, the ESC, and the battery are established, respectively.

A. Propeller Modeling

For a multicopter, fixed-pitch propellers are often used. Propeller performance depends on its thrust T (N) and torque M (N · m). Referring to [16] and [17], they are expressed as

$$T = C_T \rho \left(\frac{N}{60} \right)^2 D_p^4 \quad (1)$$

$$M = C_M \rho \left(\frac{N}{60} \right)^2 D_p^5. \quad (2)$$

Here, the air density ρ (kg/m³), which varies with respect to the local altitude h (m) and the temperature T_t (°C), is written as

$$\rho = \frac{273p}{101325(273 + T_t)} \rho_0 \quad (3)$$

where the standard air density $\rho_0 = 1.293$ kg/m³ (0 °C, 273 K). The atmospheric pressure p (Pa) is obtained as [18]

$$p = p_0 \left(1 - 0.0065 \frac{h}{273 + T_t} \right)^{5.2561}. \quad (4)$$

The height of a multicopter varies slightly while performing a task. So, h and T_t are treated as constants in the following performance evaluation. The remaining task in propeller modeling is to find the parameters C_T and C_M in (1) and (2). To make things clearer, they are expressed as

$$\begin{aligned} C_T &= f_{C_T}(\Theta_p) \\ C_M &= f_{C_M}(\Theta_p) \end{aligned} \quad (5)$$

where Θ_p is the parameter set as in Table I. The detailed procedure to obtain $f_{C_T}(\Theta_p)$ and $f_{C_M}(\Theta_p)$ is shown in Appendix A, given as

$$\begin{aligned} f_{C_T}(\Theta_p) &\triangleq 0.25\pi^3 \lambda \zeta^2 B_p K_0 \frac{\varepsilon \arctan \frac{H_p}{\pi D_p} - \alpha_0}{\pi A + K_0} \\ f_{C_M}(\Theta_p) &\triangleq \frac{1}{8A} \pi^2 C_d \zeta^2 \lambda B_p^2 \end{aligned} \quad (6)$$

where

$$C_d = C_{fd} + \frac{\pi A K_0^2 \left(\varepsilon \arctan \frac{H_p}{\pi D_p} - \alpha_0 \right)^2}{e (\pi A + K_0)^2}. \quad (7)$$

The parameters $A, \varepsilon, \lambda, \zeta, e, C_{fd}$, and α_0 , which are not reflected in Table I, are explained in Appendix A. According to experimental results and the relevant literature [19, p. 150/151/174], [20, p. 62], [21, p. 43], [22], it is suggested that the values of these parameters in (6) are taken as

$$\begin{aligned} A &= 5 \sim 8, \varepsilon = 0.85 \sim 0.95, \lambda = 0.7 \sim 0.9, \\ \zeta &= 0.4 \sim 0.7, e = 0.7 \sim 0.9, C_{fd} = 0.015, \\ \alpha_0 &= -\frac{\pi}{36} \sim 0, K_0 = 6.11. \end{aligned} \quad (8)$$

To verify the proposed modeling method, the experimental data provided on the website of APC propellers³ are used for comparison. The parameters in (8) are chosen as $A = 5, \varepsilon = 0.85, \lambda = 0.75, \zeta = 0.55, e = 0.83, C_{fd} = 0.015, \alpha_0 = 0$, and $K_0 = 6.11$. The other parameters for propellers in Table I are taken directly from the model parameters given by APC. The results are shown in Fig. 2. It can be clearly observed that the results of the theoretical model (6) match well with the experimental data.

In practice, it is impossible to determine the values of parameters in (8) to match all kinds of propellers. After comprehensive consideration of various propellers from different

³The data are from <https://www.apcprop.com/>.

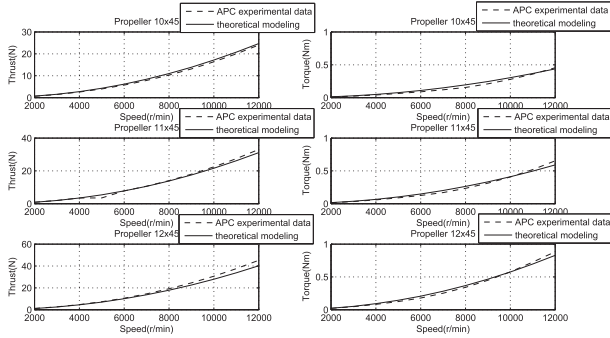


Fig. 2. Lift characteristics and drag characteristics model verification.

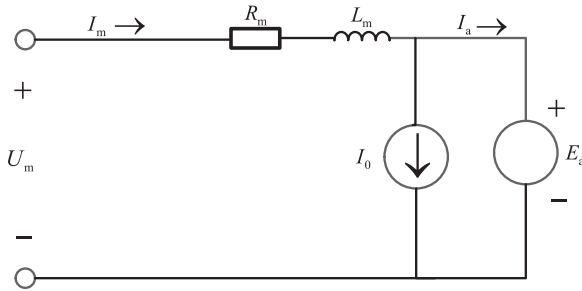


Fig. 3. Equivalent motor model. Here, U_m is the equivalent supply voltage (V), I_m is the equivalent motor input current (A), E_a is the back-electromotive force (V), R_m is the armature resistance (Ω), and L_m is the armature inductance (H). I_0 is the no-load current required to overcome mechanical friction in the motor and drive train, as well as magnetic hysteresis and eddy current losses in the motor, and is approximately a constant at a certain motor speed [23]. And $I_a = I_m - I_0$ helps produce the electromagnetic torque. Here, the armature inductance L_m and the transient process caused by switching elements are neglected.

manufacturers, in the following tests, $A = 5$, $\varepsilon = 0.85$, $\lambda = 0.75$, $\zeta = 0.5$, $e = 0.83$, $C_{fd} = 0.015$, $\alpha_0 = 0$, and $K_0 = 6.11$ are used as nominal values.

B. Motor Modeling

Nowadays, the electric motors used in multicopters are brushless dc motors. A brushless dc motor is a synchronous three-phase permanent magnet motor, which can be modeled as a permanent magnet dc motor. Its equivalent circuit is shown in Fig. 3 [12].

The motor modeling aims to obtain U_m and I_m from N , M , and Θ_m , where N and M are obtained in Section IV-A and Θ_m is shown in Table I. For clarity, they are expressed as

$$\begin{aligned} U_m &= f_{U_m}(\Theta_m, M, N) \\ I_m &= f_{I_m}(\Theta_m, M, N). \end{aligned} \quad (9)$$

The detailed procedure to obtain $f_{U_m}(\Theta_m, M, N)$ and $f_{I_m}(\Theta_m, M, N)$ is shown in Appendix B, given as

$$\begin{aligned} f_{U_m}(\Theta_m, M, N) &\triangleq R_m \left(\frac{MK_{V0}U_{m0}}{9.55(U_{m0} - I_{m0}R_m)} + I_{m0} \right) \\ &+ \frac{U_{m0} - I_{m0}R_m}{K_{V0}U_{m0}} N \end{aligned}$$

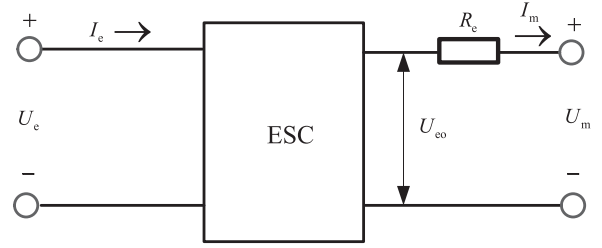


Fig. 4. ESC model.

$$f_{I_m}(\Theta_m, M, N) \triangleq \frac{MK_{V0}U_{m0}}{9.55(U_{m0} - I_{m0}R_m)} + I_{m0}. \quad (10)$$

C. ESC Modeling

An ESC is a device external to the motor that electronically performs the commutation achieved mechanically in brush motors. The ESC converts the dc voltage of the battery pack to a three-phase alternating signal, which is synchronized with the rotation of the rotor and applied to armature windings. ESCs regulate motor speed within a range depending on the load and battery voltage. An equivalent circuit of the ESC is shown in Fig. 4.

The ESC modeling aims to obtain U_e and I_e by using U_m , I_m , Θ_e , and Θ_b , where U_m and I_m are obtained in Section IV-B and Θ_e and Θ_b are shown in Table I. For clarity, they are expressed as

$$\begin{aligned} \sigma &= f_{\sigma}(\Theta_e, U_m, I_m, U_b) \\ I_e &= f_{I_e}(\sigma, I_m) \\ U_e &= f_{U_e}(\Theta_b, I_e). \end{aligned} \quad (11)$$

As shown in Fig. 4, U_{eo} is the equivalent dc voltage, given by

$$U_{eo} = U_m + I_m R_e. \quad (12)$$

Based on (12), the duty cycle σ is obtained as [24]

$$\sigma = \frac{U_{eo}}{U_e} \approx \frac{U_{eo}}{U_b} \quad (13)$$

where $\sigma \in [0, 1]$. From the perspective of power electronics, since the average motor voltage over a commutating sequence is modulated by σ , the duty cycle effectively introduces an integrated dc-dc buck converter. As a result, the ESC input current is [24]

$$I_e = \sigma I_m \quad (14)$$

which is limited by

$$I_e \leq I_{e\text{Max}}. \quad (15)$$

The ESC voltage is supplied by the battery pack, given by

$$U_e = U_b - I_b R_b \quad (16)$$

where I_b is the battery current. For a multicopter, the number of ESCs is equal to the number of rotors, so

$$I_b = n_r I_e + I_{\text{control}} \quad (17)$$

where I_{control} is the current supplied to the flight controller, usually, $I_{\text{control}} \approx 1$ A. From the above, the functions in (11) are expressed as

$$f_{\sigma}(\Theta_e, U_m, I_m, U_b) \triangleq \frac{U_m + I_m R_e}{U_b} \quad (18)$$

$$f_{I_e}(\sigma, I_m) \triangleq \sigma I_m \quad (19)$$

$$f_{U_e}(\Theta_b, I_b) \triangleq U_b - I_b R_b. \quad (20)$$

D. Battery Modeling

The battery model mainly aims to obtain the time of endurance T_b (min) by using I_b and Θ_b , where I_b is expressed in (17) and Θ_b is shown in Table I. For clarity, the model is expressed in an abstract function as

$$T_b = f_{T_b}(\Theta_b, I_b). \quad (21)$$

The battery discharge process is simplified so that the battery voltage retains constant and the battery capacity decreases linearly. Thus, the model $f_{T_b}(\Theta_b, I_b)$ is

$$f_{T_b}(\Theta_b, I_b) \triangleq \frac{C_b - C_{\min}}{I_b} \cdot \frac{60}{1000} \quad (22)$$

where C_{\min} is the minimum capacity of a battery set according to the safety margin. Generally, it can be chosen from the range of $0.15C_b - 0.2C_b$. It should be noted that C_b and C_{\min} have the unit of mAh, while I_b has the unit of A and T_b has the unit of min. This is the reason why the constant $60/1000$ is introduced into (22). The battery current has to meet the following constraint:

$$I_b \leq C_b K_b. \quad (23)$$

IV. PERFORMANCE EVALUATION

So far, the propulsion system modeling is completed. In this section, Problems 1–4 are going to be investigated. Before evaluating the performance, a virtual multicopter is defined here. Its weight is G and it has n_r propulsors. This implies n_r motors and ESCs are required. The altitude of the multicopter is h and the temperature is T_t . The parameters related to its propulsion system have the same notations shown in Table I for simplicity.

A. Solution to Problem 1

In the hover mode, the sum of thrusts provided by n_r propellers should be equal to the weight of the multicopter G . Thus, the thrust provided by a single propeller is

$$T^* = \frac{G}{n_r}. \quad (24)$$

According to (1), (2), and T^* obtained in (24), the motor speed and propeller torque are derived as

$$N^* = 60 \sqrt{\frac{T^*}{\rho D_p^4 f_{C_T}(\Theta_p)}} \quad (25)$$

$$M^* = \rho D_p^5 f_{C_M}(\Theta_p) \left(\frac{N^*}{60}\right)^2.$$

TABLE II
EXAMPLE FOR PROBLEM 1

Environment	$h = 10$ m, $T_t = 25$ °C
Basic Parameters	$G = 14.7$ N > $G_p + G_e + G_b + G_m$, $n_r = 4$
Components	$\Theta_p = \{D_p = 10$ in, $H_p = 4.5$ in, $B_p = 2$, $G_p\}$ $\Theta_m = \{K_{V0} = 890$ r/min/V, $I_{m \text{ Max}} = 19$ A, $I_{m0} = 0.5$ A, $U_{m0} = 10$ V, $R_m = 0.101$ Ω , $G_m\}$ $\Theta_e = \{I_{e \text{ Max}} = 30$ A, $R_e = 0.008$ Ω , $G_e\}$ $\Theta_b = \{C_b = 5000$ mAh, $R_b = 0.01$ Ω , $U_b = 12$ V, $K_b = 45$ C, $G_b\}$
Other parameters	$A = 5$, $\varepsilon = 0.85$, $\lambda = 0.75$, $\zeta = 0.5$, $e = 0.83$, $C_{fd} = 0.015$, $\alpha_0 = 0$, $K_0 = 6.11$, $C_1 = 3$, $C_2 = 1.5$, $C_{\min} = 0.2C_b$
Results	$T_{\text{loiter}} = 15.8$ min, $\sigma = 54.6\%$, $I_e = 3.6$ A, $U_e = 11.8$ V, $I_b = 15.2$ A, $N = 5223$ r/min

Then, substituting M^* and N^* into (10) yields

$$U_m^* = f_{U_m}(\Theta_m, M^*, N^*)$$

$$I_m^* = f_{I_m}(\Theta_m, M^*, N^*). \quad (26)$$

In the next stage, by using the given parameters of the ESC and the battery in Table I, the duty cycle and the ESC input current and voltage are obtained according to (18)–(20) as

$$\sigma^* = f_{\sigma}(\Theta_e, U_m^*, I_m^*, U_b)$$

$$I_e^* = f_{I_e}(\sigma^*, I_m^*)$$

$$U_e^* = f_{U_e}(\Theta_b, I_b^*). \quad (27)$$

Consequently, according to (17), the battery current is

$$I_b^* = n_r I_e^* + I_{\text{control}}. \quad (28)$$

Finally, the hovering endurance is calculated by (22) as

$$T_{\text{loiter}}^* = f_{T_b}(\Theta_b, I_b^*). \quad (29)$$

An example for Problem 1 is given in Table II, where the adopted parameters and evaluation results are shown.

Remark 1: Generally, in the hover mode, the duty cycle is expected to be about 50% in order to ensure a sufficient control margin.

B. Solution to Problem 2

In the maximum thrust mode, the duty cycle $\sigma^* = 1$ which implies that the equivalent motor voltage U_m^* reaches its peak. First, I_m^* , U_m^* , M^* , and N^* are solved by using the following equations:

$$f_{\sigma}(\Theta_e, U_m, I_m, U_b) = 1$$

$$M - \rho D_p^5 f_{C_M}(\Theta_p) \left(\frac{N}{60}\right)^2 = 0$$

$$U_m - f_{U_m}(\Theta_m, M, N) = 0$$

$$I_m - f_{I_m}(\Theta_m, M, N) = 0 \quad (30)$$

which are derived from (2), (10), and (18). Substituting I_m^* into (19) yields I_e^* . Then, based on (20) and (17), U_e^* and I_b^* are

TABLE III
EXAMPLE FOR PROBLEM 2

Environment	$h = 10 \text{ m}, T_t = 25^\circ \text{C}$
Basic Parameters	$G = 14.7 \text{ N} > G_p + G_e + G_b + G_m, n_r = 4$
Components	$\Theta_p = \{D_p = 10 \text{ in}, H_p = 4.5 \text{ in}, B_p = 2, G_p\}$ $\Theta_m = \{K_{V0} = 890 \text{ r/min/V}, I_{m \text{ Max}} = 19 \text{ A}, I_{m0} = 0.5 \text{ A},$ $U_{m0} = 10 \text{ V}, R_m = 0.101 \Omega, G_m\}$ $\Theta_e = \{I_{e \text{ Max}} = 30 \text{ A}, R_e = 0.008 \Omega, G_e\}$ $\Theta_b = \{C_b = 5000 \text{ mAh}, R_b = 0.01 \Omega,$ $U_b = 12 \text{ V}, K_b = 45 \text{ C}, G_b\}$
Other parameters	$A = 5, \varepsilon = 0.85, \lambda = 0.75, \zeta = 0.5, e = 0.83,$ $C_{fd} = 0.015, \alpha_0 = 0, K_0 = 6.11,$ $C_1 = 3, C_2 = 1.5, C_{\text{min}} = 0.2 C_b$
Results	$I_e = 16.5 \text{ A}, U_e = 11.3 \text{ V}, I_b = 66.2 \text{ A},$ $N = 8528 \text{ r/min}, \eta = 77.1\%$

obtained as

$$\begin{aligned} I_e^* &= f_{I_e}(1, I_m^*) \\ I_b^* &= n_r I_e^* + I_{\text{control}} \\ U_e^* &= f_{U_e}(\Theta_b, I_b^*). \end{aligned} \quad (31)$$

The system efficiency is the ratio between the propeller output power and the battery power, which is calculated by

$$\eta^* = \frac{\frac{2\pi}{60} n_r M^* N^*}{U_b I_b^*}. \quad (32)$$

An example for Problem 2 is given in Table III, where the adopted parameters and evaluation results are shown.

C. Solution to Problem 3

The maximum load and the maximum pitch are closely related to the safety of a multicopter, which should be taken into account. In order to ensure a sufficient control margin, the maximum load is not estimated in the case of the maximum thrust, i.e., $\sigma = 1$. Generally, a maximum duty cycle σ of an ESC between 0.7 and 0.9 is acceptable when a multicopter hovers in the air. In the paper, $\sigma^* = 0.8$ is taken to estimate the maximum load. Similar to Problem 2, according to (2), (10), and (18), I_m^*, U_m^*, M^* , and N^* are solved by the following equations:

$$\begin{aligned} f_\sigma(\Theta_e, U_m, I_m, U_b) &= 0.8 \\ M - \rho D_p^5 f_{C_M}(\Theta_p) \left(\frac{N}{60}\right)^2 &= 0 \\ U_m - f_{U_m}(\Theta_m, M, N) &= 0 \\ I_m - f_{I_m}(\Theta_m, M, N) &= 0. \end{aligned} \quad (33)$$

Then, according to (1), the produced propeller thrust T^* is calculated as

$$T^* = \rho D_p^4 f_{C_T}(\Theta_p) \left(\frac{N^*}{60}\right)^2. \quad (34)$$

Therefore, the maximum load is

$$G_{\text{maxload}}^* = n_r T^* - G. \quad (35)$$

TABLE IV
EXAMPLE FOR PROBLEM 3

Environment	$h = 10 \text{ m}, T_t = 25^\circ \text{C}$
Basic Parameters	$G = 14.7 \text{ N} > G_p + G_e + G_b + G_m, n_r = 4$
Components	$\Theta_p = \{D_p = 10 \text{ in}, H_p = 4.5 \text{ in}, B_p = 2, G_p\}$ $\Theta_m = \{K_{V0} = 890 \text{ r/min/V}, I_{m \text{ Max}} = 19 \text{ A}, I_{m0} = 0.5 \text{ A},$ $U_{m0} = 10 \text{ V}, R_m = 0.101 \Omega, G_m\}$ $\Theta_e = \{I_{e \text{ Max}} = 30 \text{ A}, R_e = 0.008 \Omega, G_e\}$ $\Theta_b = \{C_b = 5000 \text{ mAh}, R_b = 0.01 \Omega,$ $U_b = 12 \text{ V}, K_b = 45 \text{ C}, G_b\}$
Other parameters	$A = 5, \varepsilon = 0.85, \lambda = 0.75, \zeta = 0.5, e = 0.83,$ $C_{fd} = 0.015, \alpha_0 = 0, K_0 = 6.11,$ $C_1 = 3, C_2 = 1.5, C_{\text{min}} = 0.2 C_b$
Results	$G_{\text{maxload}} = 1.32 \text{ kg}, \theta_{\text{max}} = 1.01 \text{ rad} (57.9^\circ)$

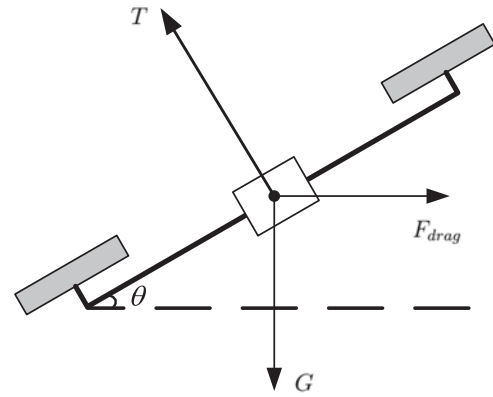


Fig. 5. Multicopter in forward flight.

In addition, the maximum pitch is given by

$$\theta_{\text{max}}^* = \arccos \frac{G}{n_r T^*}. \quad (36)$$

An example for Problem 3 is given in Table IV, where the adopted parameters and evaluation results are shown.

D. Solution to Problem 4

Maximum forward flight speed and maximum flight distance are the key performance indices, which both designers and users are concerned about. The solution to Problem 4 is derived through the following three steps. First, the forward flight speed is solved for. Second, the flight distance is obtained. Finally, the optimizations are conducted.

1) *Forward Flight Speed*: The multicopter force is shown in Fig. 5. The first step is to solve for the forward flight speed under the given pitch angle θ of a multicopter.

The detailed procedure to obtain $V(\theta)$ is shown in Appendix C, given as

$$V(\theta) = \sqrt{\frac{2G \tan \theta}{\rho S [C_1 (1 - \cos^3 \theta) + C_2 (1 - \sin^3 \theta)]}}. \quad (37)$$

where the parameters S, C_1 , and C_2 are explained in Appendix C.

TABLE V
EXAMPLE FOR PROBLEM 4

Environment	$h = 10 \text{ m}, T_t = 25 \text{ }^\circ\text{C}$
Basic Parameters	$G = 14.7 \text{ N} > G_p + G_e + G_b + G_m, n_r = 4$
Components	$\Theta_p = \{D_p = 10 \text{ in}, H_p = 4.5 \text{ in}, B_p = 2, G_p\}$ $\Theta_m = \{K_{V0} = 890 \text{ r/min/V}, I_{m \text{ Max}} = 19 \text{ A}, I_{m0} = 0.5 \text{ A},$ $U_{m0} = 10 \text{ V}, R_m = 0.101 \text{ } \Omega, G_m\}$ $\Theta_e = \{I_{e \text{ Max}} = 30 \text{ A}, R_e = 0.008 \text{ } \Omega, G_e\}$ $\Theta_b = \{C_b = 5000 \text{ mAh}, R_b = 0.01 \text{ } \Omega,$ $U_b = 12 \text{ V}, K_b = 45 \text{ C}, G_b\}$
Other parameters	$A = 5, \varepsilon = 0.85, \lambda = 0.75, \zeta = 0.5, e = 0.83,$ $C_{fd} = 0.015, \alpha_0 = 0, K_0 = 6.11,$ $C_1 = 3, C_2 = 1.5, C_{\min} = 0.2C_b$
Results	$V_{\text{max}} = 11.2 \text{ m/s}, Z_{\text{max}} = 6021.4 \text{ m}$

2) *Flight Distance*: The second step is to solve for the flight distance. According to (1), the motor speed $N(\theta)$ is given by

$$N(\theta) = 60 \sqrt{\frac{G}{\rho C_T D_p^4 n_r \cos \theta}}. \quad (38)$$

Consequently, through (2), $M(\theta)$ is obtained as

$$M(\theta) = \frac{G C_M D_p}{C_T n_r \cos \theta}. \quad (39)$$

Finally, the total flight time $T_{fly}(\theta)$ is calculated through the equations as

$$\begin{aligned}
 U_m(\theta) &= f_{U_m}(\Theta_m, M(\theta), N(\theta)) \\
 I_m(\theta) &= f_{I_m}(\Theta_m, M(\theta), N(\theta)) \\
 \sigma(\theta) &= f_\sigma(\Theta_e, U_m(\theta), I_m(\theta), U_b) \\
 I_e(\theta) &= f_{I_e}(\sigma(\theta), I_m(\theta)) \\
 I_b(\theta) &= n_r I_e(\theta) + I_{\text{control}} \\
 T_{fly}(\theta) &= f_{T_b}(\Theta_b, I_b(\theta))
 \end{aligned} \quad (40)$$

where (10), (17), (18), (19), and (22) are utilized. With the total flight time $T_{fly}(\theta)$, the flight distance $Z(\theta)$ is

$$Z(\theta) = 60V(\theta) T_{fly}(\theta). \quad (41)$$

3) *Optimization*: The third step is to conduct the optimization. In order to find the maximum forward flight speed V_{max} , an optimization problem is formulated as

$$V_{\text{max}} = \max_{\theta \in [0, \theta_{\text{max}}]} V(\theta) \quad (42)$$

where $V(\theta)$ is denoted by (37) and θ_{max} is solved in Problem 3. Furthermore, in order to find the maximum flight distance Z_{max} , an optimization problem is formulated as

$$Z_{\text{max}} = \max_{\theta \in [0, \theta_{\text{max}}]} 60V(\theta) T_{fly}(\theta) \quad (43)$$

where $Z(\theta)$ is obtained by (41). Both (42) and (43) can be solved through the numerical traversal algorithm. By changing θ change from 0 to θ_{max} , the global optimal solution is obtained.

An example for Problem 4 is given in Table V, where the adopted parameters and evaluation results are shown.

V. EXPERIMENTS

In order to demonstrate the effectiveness of the propulsion system model, the results provided by the www.ecalc.ch/ are used for comparison purpose. Moreover, the performances of a commercial quadcopter given by the manufacturers are also verified using our method.

A. Comparisons With www.ecalc.ch/

www.ecalc.ch/ is a frequently visited website (more than 5 million visits since February 2010) providing flight performance evaluation for multicopters. It is claimed that the evaluation results are reliable. Comparisons with www.ecalc.ch/ can verify the evaluation results to a certain extent. Here, three arbitrary multicopters are chosen to conduct the comparisons, the detailed parameters of which are shown in Table VI. The corresponding comparative results are illustrated in Table VII. It is indicated that there is a significant similarity between the website calculations and the proposed evaluation [25], [26].

B. Comparison With a Commercial Multicopter

The quadcopter DJI Inspire I is considered in this section. Table VIII shows detailed parameters of the product retrieved from <http://www.dji.com/cn/product/inspire-1>. The evaluation results, shown in Table IX, are compared with the corresponding data from the DJI website.⁴ The results demonstrate that the results from evaluations are close to the provided data.⁵

C. Comparison With Real Experiment Results

To verify the effectiveness of the proposed method further, some indoor experiments are conducted so that various parameters can be measured easily. The schematic diagram of experimental equipment is shown in Fig. 6. For simplicity, hovering endurance can be regarded as a representative index to reflect the accuracy of the proposed method. In the experiments, two sets of parameters of the components are given in Table X.

From Fig. 6, it is observed that the thrust provided by a propeller (i.e., T/n_r in Fig. 5) is measured through electronic scale, the propeller speed is measured through laser tachometer, the ESC input current is measured through current shunt, the battery voltage is measured through electronic multimeter, and the throttle command (duty cycle) is read from the RC transmitter directly. By regulating the throttle, different motor speeds are obtained. As a result, the relationship between the thrust and the motor speed is calculated, and the relationship between the ESC input current and the motor speed is established. All of these are compared with the results of the proposed method, as shown in Figs. 7 and 8. The results show that the curves obtained by the proposed method and the experiment are similar.

⁴The www.ecalc.ch/ does not provide a motor with the same brand and model.

⁵As the source of data from the DJI website is unknown, when $C_{\min} = 0.15C_b$ is taken to estimate the hovering endurance, $T_{\text{loiter}} = 17.1 \text{ min}$; when $C_{\min} = 0.2C_b$ is taken to estimate the hovering endurance, $T_{\text{loiter}} = 16.1 \text{ min}$.

TABLE VI
PARAMETERS OF MULTICOPTER 1–3

Multicopter 1	Environment	$h = 10 \text{ m}, T_t = 25^\circ\text{C}$
	Basic Parameters	$G = 14.7 \text{ N} > G_p + G_e + G_b + G_m, n_r = 4$
	Components	$\Theta_p = \{D_p = 10 \text{ in}, H_p = 4.5 \text{ in}, B_p = 2, G_p\}$ $\Theta_m = \{K_{V0} = 890 \text{ r/min/V}, I_{m \text{ Max}} = 19 \text{ A}, I_{m0} = 0.5 \text{ A}, U_{m0} = 10 \text{ V},$ $R_m = 0.101 \Omega, G_m\}$ $\Theta_e = \{I_{e \text{ Max}} = 30 \text{ A}, R_e = 0.008 \Omega, G_e\}$
	Other Parameters	$\Theta_b = \{C_b = 5000 \text{ mAh}, R_b = 0.0078 \Omega, U_b = 11.1 \text{ V}, K_b = 45 \text{ C}, G_b\}$ $A = 5, \varepsilon = 0.85, \lambda = 0.75, \zeta = 0.5, e = 0.83, C_{fd} = 0.015, \alpha_0 = 0,$ $K_0 = 6.11, C_1 = 3, C_2 = 1.5, C_{\text{min}} = 0.2C_b$
Multicopter 2	Environment	$h = 10 \text{ m}, T_t = 25^\circ\text{C}$
	Basic Parameters	$G = 28.763 \text{ N} > G_p + G_e + G_b + G_m, n_r = 4$
	Components	$\Theta_p = \{D_p = 13 \text{ in}, H_p = 4.5 \text{ in}, B_p = 2, G_p\}$ $\Theta_m = \{K_{V0} = 415 \text{ r/min/V}, I_{m \text{ Max}} = 22 \text{ A}, I_{m0} = 0.3 \text{ A}, U_{m0} = 10 \text{ V},$ $R_m = 0.2425 \Omega, G_m\}$ $\Theta_e = \{I_{e \text{ Max}} = 30 \text{ A}, R_e = 0.008 \Omega, G_e\}$
	Other Parameters	$\Theta_b = \{C_b = 5500 \text{ mAh}, R_b = 0.0114 \Omega, U_b = 22.2 \text{ V}, K_b = 55 \text{ C}, G_b\}$ $A = 5, \varepsilon = 0.85, \lambda = 0.75, \zeta = 0.5, e = 0.83, C_{fd} = 0.015, \alpha_0 = 0,$ $K_0 = 6.11, C_1 = 3, C_2 = 1.5, C_{\text{min}} = 0.2C_b$
Multicopter 3	Environment	$h = 10 \text{ m}, T_t = 25^\circ\text{C}$
	Basic Parameters	$G = 29.4 \text{ N} > G_p + G_e + G_b + G_m, n_r = 6$
	Components	$\Theta_p = \{D_p = 12 \text{ in}, H_p = 5.5 \text{ in}, B_p = 2, G_p\}$ $\Theta_m = \{K_{V0} = 480 \text{ r/min/V}, I_{m \text{ Max}} = 20 \text{ A}, I_{m0} = 0.4 \text{ A}, U_{m0} = 10 \text{ V},$ $R_m = 0.178 \Omega, G_m\}$ $\Theta_e = \{I_{e \text{ Max}} = 40 \text{ A}, R_e = 0.006 \Omega, G_e\}$
	Other Parameters	$\Theta_b = \{C_b = 5000 \text{ mAh}, R_b = 0.0168 \Omega, U_b = 22.2 \text{ V}, K_b = 35 \text{ C}, G_b\}$ $A = 5, \varepsilon = 0.85, \lambda = 0.75, \zeta = 0.5, e = 0.83, C_{fd} = 0.015, \alpha_0 = 0,$ $K_0 = 6.11, C_1 = 3, C_2 = 1.5, C_{\text{min}} = 0.2C_b$

TABLE VII
PERFORMANCE OF MULTICOPTER 1–3

Mode	Performance	Vehicle 1		Vehicle 2		Vehicle 3	
		Ecalc	Proposed	Ecalc	Proposed	Ecalc	Proposed
Hover Mode	Hovering Endurance	13.6 min	14.6 min	14.1 min	13.9 min	15.1 min	15.4 min
	Duty Cycle	62%	59.0%	62%	61.3%	46%	43.3%
	Propeller Speed	5297 r/min	5223 r/min	4785 r/min	4923 r/min	4222 r/min	4151 r/min
	ESC Current	4.4 A	3.8 A	4.7 A	4.5 A	2.8 A	2.4 A
Max Thrust Mode	ESC Current	12.1 A	14.9 A	13.1 A	15.9 A	16.6 A	19.8 A
	Propeller Speed	8276 r/min	8066 r/min	7493 r/min	7315 r/min	8269 r/min	8003 r/min
	System Efficiency	80.4%	78.5%	79.0%	77.3%	74.6%	73.1%
Flight Mode	Maximum Load	0.964 kg	0.99 kg	1.969 kg	1.60 kg	4.941 kg	5.14 kg
	Maximum Pitch	52°	53.0°	53°	49.6°	68°	68.4°
	Maximum Speed	10.5 m/s	10.2 m/s	9.7 m/s	9.4 m/s	15.3 m/s	13.7 m/s
	Maximum Distance	N/A	5662.3 m	N/A	5128.6 m	N/A	5819.6 m

TABLE VIII
DJI INSPIRE I PARAMETERS

Environment	$h = 10 \text{ m}, T = 25^\circ\text{C}$
Basic Parameters	$G = 28.763 \text{ N}, n_r = 4$
Motor	DJI 3510 ($K_{V0} = 350 \text{ r/min/V}, R_m = 0.21 \Omega,$ $I_{m \text{ Max}} = 20 \text{ A}, I_{m0} = 0.3 \text{ A}, U_{m0} = 10 \text{ V}$)
Propeller	DJI 1345 ($D_p = 13 \text{ in}, H_p = 4.5 \text{ in}, B_p = 2$)
ESC	$I_{e \text{ Max}} = 20 \text{ A}, R_e = 0.02 \Omega$
Battery	$C_b = 5700 \text{ mAh}, U_b = 24 \text{ V}, R_b = 0.12 \Omega$

TABLE IX
COMPARISON WITH DJI INSPIRE I

Performance	DJI	eCalc Website	Proposed
Hovering Endurance	18 min	N/A	17.1 min
Maximum Load	0.465 kg	N/A	0.55 kg
Maximum Pitch	35°	N/A	32.7°

Furthermore, in order to simulate the hover mode of a multicopter (i.e., $\theta = 0$ in Fig. 5), the thrust produced by the propeller in the experiments can be assumed as G/n_r . If a virtual vehi-

cle weight G is given, the needed thrust is determined and can be obtained by regulating the throttle. The equivalent hovering endurance of a multicopter is equal to the discharge time of the battery. The experimental results of the hovering endurance are compared with the values calculated by the proposed method, as shown in Table XI.

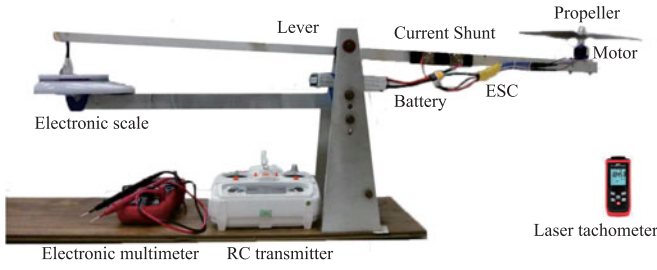


Fig. 6. Experimental equipments.

TABLE X
PARAMETERS OF EXPERIMENT COMPONENTS

Test	Environment	$h = 50 \text{ m}, T_t = 20^\circ \text{C}$
Test 1	Propeller	APC $10 \times 45\text{MR}$ ($D_p = 10$ in, $H_p = 4.5$ in, $B_p = 2$)
	Motor	Sunnysky Angel A2212 ($K_{V0} = 980$ r/min/V, $R_m = 0.12 \Omega$, $I_{m \text{ Max}} = 20$ A, $I_{m0} = 0.5$ A, $U_{m0} = 10$ V)
	ESC	$I_{e \text{ Max}} = 30$ A, $R_e = 0.008 \Omega$
	Battery	ACE ($C_b = 4000$ mAh, $U_b = 12$ V, $R_b = 0.016 \Omega$, $K_b = 25$ C)
	Others	$A = 5$, $\varepsilon = 0.85$, $\lambda = 0.75$, $\zeta = 0.5$, $e = 0.83$, $C_{fd} = 0.015$, $\alpha_0 = 0$, $K_0 = 6.11$, $C_{min} = 0.2C_b$
Test 2	Environment	$h = 50 \text{ m}, T_t = 20^\circ \text{C}$
	Propeller	T-MOTOR 30×10.5 ($D_p = 30$ in, $H_p = 10.5$ in, $B_p = 2$)
	Motor	T-MOTOR U12 ($K_{V0} = 90$ r/min/V, $R_m = 0.047 \Omega$, $I_{m \text{ Max}} = 50$ A, $I_{m0} = 1.2$ A, $U_{m0} = 10$ V)
	ESC	$I_{e \text{ Max}} = 80$ A, $R_e = 0.0035 \Omega$
	Battery	ACE ($C_b = 22\,000$ mAh, $U_b = 48$ V, $R_b = 0.01 \Omega$, $K_b = 25$ C)
	Others	$A = 5$, $\varepsilon = 0.85$, $\lambda = 0.75$, $\zeta = 0.5$, $e = 0.83$, $C_{fd} = 0.015$, $\alpha_0 = 0$, $K_0 = 6.11$, $C_{min} = 0.2C_b$

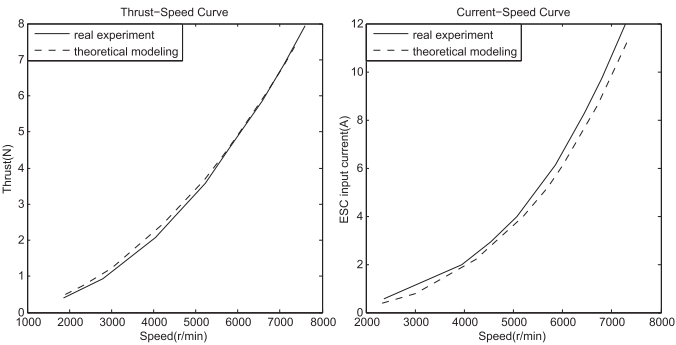


Fig. 7. Test 1: Thrust-speed curve and current-speed curve.

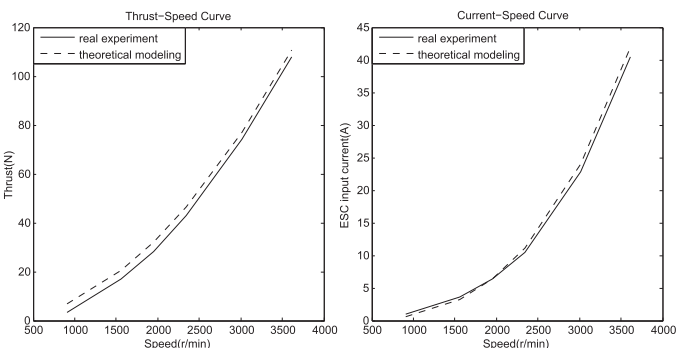


Fig. 8. Test 2: Thrust-speed curve and current-speed curve.

TABLE XI
VALUES OF HOVERING ENDURANCE

Test	Virtual Multicopter Environment Components	$G = 14.7 \text{ N}, n_r = 4$ See Table X See Table X
Test 1	Hovering Endurance	Experiment 12.4 min Proposed 12.2 min
	Virtual Multicopter Environment Components	$G = 294 \text{ N}, n_r = 6$ See Table X See Table X
Test 2	Hovering Endurance	Experiment 12.3 min Proposed 12 min

Since the flight controller is not used, the flight controller current I_{control} is not included in the experiments. As a result, the measurement value of the hovering endurance is a bit greater than the calculated one for each test, respectively. This result is reasonable.

D. Website

A performance evaluation website www.flyeval.com for multicopters is established by the authors in February 2016. Users can perform the flight evaluations mentioned above after providing the airframe configuration parameters, the environment parameters, and the propulsion system parameters. In addition, some other performance indices are given on the website.⁶

VI. CONCLUSION

Multicopter performance evaluation is of significant importance for a multicopter design. In this paper, models of the propulsion system are established, including the propeller, the motor, the ESC, and the battery. Based on these models, performances of a multicopter are evaluated in different modes, such as the hover mode, the maximum thrust mode, and the forward flight mode. All the comparisons demonstrate the effectiveness of the proposed evaluation method. In real flight, different control methods will lead to different energy consumption [27], [28]. In this paper, the evaluation is performed for the energy conversion at steady state rather than during all dynamic process. Generally, the proposed evaluation at the steady state will dominate. However, it is still an interesting problem for studying an appropriate method to save energy in the future. The major contributions of this paper are as follows.

- 1) A comprehensive evaluation method of multicopter performance proposed, including evaluation in the hover mode, in the maximum thrust mode and in the forward flight mode.
- 2) The evaluation method only required component parameters provided by device manufacturers.

⁶The algorithm used in the website will be updated in a timely fashion. For example, we adopt a general propeller model as a tradeoff for the time being, but in the future, propellers from each manufacturer will have their unique model to achieve a higher accuracy.

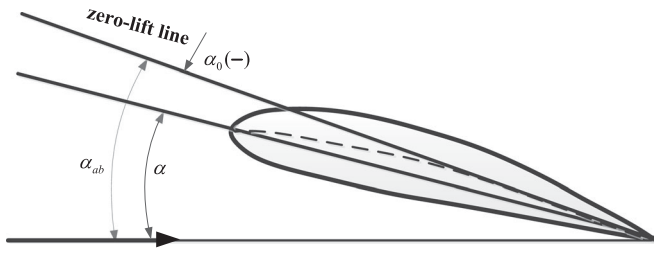


Fig. 9. Geometric and absolute angle of attack.

- 3) A website for users in the world established based on the proposed method.

APPENDIX A

PROCEDURE TO OBTAIN $f_{C_T}(\Theta_p)$ AND $f_{C_M}(\Theta_p)$

The task of this section is to give a concrete expression of $f_{C_T}(\Theta_p)$ as well as $f_{C_M}(\Theta_p)$, where Θ_p is defined in Table I.

1) *Absolute Angle of Attack α_{ab}* : It is assumed that the blade angle of a multicopter is constant along the direction of radius, given by [29, p. 40]

$$\theta = \arctan \frac{H_p}{\pi D_p} \quad (44)$$

where H_p and D_p are the parameters from Θ_p in Table I. The effective angle of attack α is

$$\alpha = \varepsilon(\theta - \phi_0) \quad (45)$$

where ε is the correction factor that arises due to downwash, and ϕ_0 is the helix angle. Considering flight characteristics of a multicopter, it is assumed $\phi_0 \approx 0$. The absolute angle of attack α_{ab} is [19, p. 136]

$$\alpha_{ab} = \alpha - \alpha_0. \quad (46)$$

The relationship among α_{ab} , α , and α_0 is shown in Fig. 9.

2) *Lift Coefficient C_l and Drag Coefficient C_d* : The lift coefficient is related to the absolute angle of attack, which is given by [19, p. 164]

$$C_l = \frac{K_0 \alpha_{ab}}{1 + K_0/\pi A} \quad (47)$$

where K_0 is chosen as $K_0 \approx 6.11$ [19, p. 151], and $A = D_p/c_p$ is the aspect ratio. Considering the downwash, A is in the range 5–8. Furthermore, the drag coefficient is given by [19, p. 174]

$$C_d = C_{fd} + \frac{1}{\pi A e} C_l^2 \quad (48)$$

where C_{fd} is the zero-lift drag coefficient, which depends on the thickness of the blade, the Reynolds number, the angle of attack, etc. The Oswald factor e is selected between 0.7 and 0.9.

3) *Thrust T and Torque M* : The blade airfoil lift is related to the aerofoil and the rotational speed, given by [29, p. 117]

$$L = \frac{1}{2} C_l \rho S_{sa} W^2 \quad (49)$$

where $S_{sa} = \frac{B_p}{2} \lambda D_p c_p$ is the blade area, in which λ is the correction coefficient, and W is the airspeed of a blade. The

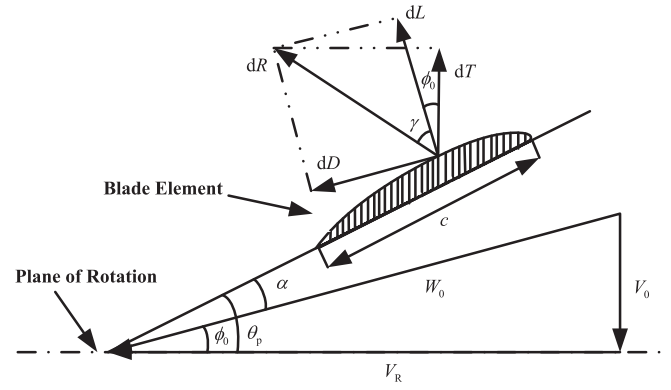


Fig. 10. Blade element force diagram.

airspeed of a blade W in flight mainly has two components: One is from the average rotor linear speed and the other is from the flight speed of a multicopter. Generally, the former is much greater than the latter. Therefore, let W be the average rotor linear speed so that

$$W \approx \pi \zeta D_p \frac{N}{60} \quad (50)$$

where $\zeta = 0.4 \sim 0.7$. According to the blade-element theory, the blade element force diagram is shown in Fig. 10. In Fig. 10, it is shown that the thrust of a multicopter is not equal to its lift. The thrust is

$$T = L \frac{\cos(\gamma + \phi_0)}{\cos(\gamma - \delta)} \quad (51)$$

where the correction angle due to the downwash effect γ is expressed as [11, p. 50]

$$\gamma = \arctan \frac{dD}{dL} = \arctan \frac{\frac{1}{2} C_d \rho W^2 c dr}{\frac{1}{2} C_l \rho W^2 c dr} = \arctan \frac{C_d}{C_l}$$

and δ is neglected because the influence of downwash has been taken into consideration in ε . Moreover, since $\phi_0 \approx 0$, $T = L$. Based on the previous results, the propeller torque is approximated as

$$M = \frac{1}{4} \rho B_p C_d W^2 S_{sa} D_p. \quad (52)$$

4) *Results*: According to (44)–(52), $f_{C_T}(\Theta_p)$ and $f_{C_M}(\Theta_p)$ are obtained as follows:

$$f_{C_T}(\Theta_p) = C_T = 0.25 \pi^3 \lambda \zeta^2 B_p K_0 \frac{\varepsilon \arctan \frac{H_p}{\pi D_p} - \alpha_0}{\pi A + K_0}$$

$$f_{C_M}(\Theta_p) = C_M = \frac{1}{8A} \pi^2 C_d \zeta^2 \lambda B_p^2 \quad (53)$$

where

$$C_d = C_{fd} + \frac{\pi A K_0^2 \left(\varepsilon \arctan \frac{H_p}{\pi D_p} - \alpha_0 \right)^2}{e (\pi A + K_0)^2}. \quad (54)$$

APPENDIX B
PROCEDURE TO OBTAIN $f_{U_m}(\Theta_m, M, N)$ AND
 $f_{I_m}(\Theta_m, M, N)$

The task of this section is to give a concrete expression of $f_{U_m}(\Theta_m, M, N)$ as well as $f_{I_m}(\Theta_m, M, N)$, where Θ_m is defined in Table I, where M is the propeller torque and N is the motor speed.

1) *Equivalent Motor Current I_m* : A brushless dc motor is modeled as a permanent magnet dc motor. According to electric machine theory, a motor's electromagnetic torque T_e is given by [30, p. 516]

$$T_e = K_T I_m \quad (55)$$

where K_T is the torque constant (N·m/A). The output torque is equal to the propeller torque, calculated as

$$M = T_e - T_0 = K_T (I_m - \hat{I}_0) \quad (56)$$

where $T_0 = K_T \hat{I}_0$ is the no-load torque and \hat{I}_0 is the no-load current in actual working state. By (56), I_m is obtained as

$$I_m = \frac{M}{K_T} + \hat{I}_0 \quad (57)$$

which is required that $I_m \leq I_{m\text{Max}}$. Usually, \hat{I}_0 and I_{m0} are quite similar. Therefore, for simplicity, let $I_{m0} = \hat{I}_0$ in practice

2) *Torque Constant K_T* : The back-electromotive force E_a is [30, p. 516]

$$E_a = K_E N \quad (58)$$

where K_E is the back-electromotive force constant. The equivalent motor voltage is [30, p. 539]

$$U_m = K_E N + I_m R_m. \quad (59)$$

The nominal no-load motor constant K_{V0} is the ratio between the no-load motor speed N_0 and the no-load motor input voltage U_0 . Consequently

$$N_0 = K_{V0} U_0. \quad (60)$$

Let $U_0 = U_{m0}$ here. Then, combining (59) with (60) results in

$$K_E = \frac{U_{m0} - I_{m0} R_m}{K_{V0} U_{m0}}. \quad (61)$$

The torque constant K_T and the back-electromotive force constant K_E have the following relationship [30, p. 516]:

$$K_T = 9.55 K_E. \quad (62)$$

Then, with (61) in hand, K_T is

$$K_T = 9.55 \frac{U_{m0} - I_{m0} R_m}{K_{V0} U_{m0}}. \quad (63)$$

3) *Results*: According to (55)–(63), $f_{U_m}(\Theta_m, M, N)$ and $f_{I_m}(\Theta_m, M, N)$ are obtained as follows:

$$\begin{aligned} f_{U_m}(\Theta_m, M, N) &= U_m = R_m \left(\frac{M K_{V0} U_{m0}}{9.55(U_{m0} - I_{m0} R_m)} + I_{m0} \right) \\ &\quad + \frac{U_{m0} - I_{m0} R_m}{K_{V0} U_{m0}} N \\ f_{I_m}(\Theta_m, M, N) &= I_m = \frac{M K_{V0} U_{m0}}{9.55(U_{m0} - I_{m0} R_m)} + I_{m0}. \end{aligned} \quad (64)$$

APPENDIX C
PROCEDURE TO OBTAIN $V(\theta)$

The task of this section is to give the expression of $V(\theta)$, where θ is the pitch angle of a multicopter. As shown in Fig. 5, equations to describe the force equilibrium in forward flight state are established as follows:

$$\begin{aligned} F_{\text{drag}}(\theta) &= G \tan \theta \\ T(\theta) &= \frac{G}{n_r \cos \theta} \end{aligned} \quad (65)$$

where $F_{\text{drag}}(\theta)$ is the drag acting on a multicopter. The drag is further expressed as [31]

$$F_{\text{drag}}(\theta) = \frac{1}{2} C_D(\theta) \rho V^2 S \quad (66)$$

where V is the forward flight speed, S is the maximum cross-sectional area, and $C_D(\theta)$ is the whole vehicle drag coefficient related to θ . Considering that θ may change in a large range (up to 90°), $C_D(\theta)$ can be approximately expressed as

$$C_D(\theta) = C_1 (1 - \cos^3 \theta) + C_2 (1 - \sin^3 \theta). \quad (67)$$

Here, C_1 and C_2 are related to the aerodynamic configuration of a multicopter, which can be estimated by computational fluid dynamics simulation software. So, the forward flight speed $V(\theta)$ is written as

$$V(\theta) = \sqrt{\frac{2G \tan \theta}{\rho S [C_1 (1 - \cos^3 \theta) + C_2 (1 - \sin^3 \theta)]}}. \quad (68)$$

REFERENCES

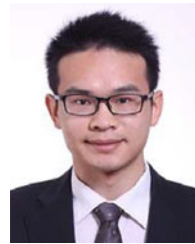
- [1] C. E. Doyle *et al.*, "An avian-inspired passive mechanism for quadrotor perching," *IEEE/ASME Trans. Mechatronics*, vol. 18, no. 2, pp. 506–517, Apr. 2013.
- [2] F. Tauro *et al.*, "Large-scale particle image velocimetry from an unmanned aerial vehicle," *IEEE/ASME Trans. Mechatronics*, vol. 20, no. 6, pp. 3269–3275, Dec. 2015.
- [3] Y. C. Choi and H. S. Ahn, "Nonlinear control of quadrotor for point tracking: Actual implementation and experimental tests," *IEEE/ASME Trans. Mechatronics*, vol. 20, no. 3, pp. 1179–1192, Jun. 2015.
- [4] R. Mahony, V. Kumar, and P. Corke, "Multirotor aerial vehicles: Modeling, estimation, and control of quadrotor," *IEEE Robot. Autom. Mag.*, vol. 19, no. 3, pp. 20–32, Sep. 2012.
- [5] S. Driessens and P. Pounds, "The triangular quadrotor: A more efficient quadrotor configuration," *IEEE Trans. Robot.*, vol. 31, no. 6, pp. 1517–1526, Dec. 2015.
- [6] O. Magnussen, G. Hovland, and M. Ottestad, "Multicopter UAV design optimization," in *Proc. IEEE/ASME 10th Int. Conf. Mechatronic Embedded Syst. Appl.*, 2014, pp. 1–6.
- [7] J. B. Brandt and M. S. Selig, "Propeller performance data at low Reynolds numbers," in *Proc. 49th AIAA Aerosp. Sci. Meeting*, 2011, pp. 2011–1255.

- [8] P. Pillay and R. Krishnan, "Modeling, simulation, and analysis of permanent-magnet motor drives. II. The brushless DC motor drive," *IEEE Trans. Ind. Appl.*, vol. 25, no. 2, pp. 274–279, Mar./Apr. 1989.
- [9] A. S. Sanca, P. J. Alsina, and J. de Jesus F Cerqueira, "Dynamic modelling of a quadrotor aerial vehicle with nonlinear inputs," in *Proc. IEEE Latin Amer. Robot. Symp.*, 2008, pp. 143–148.
- [10] O. Magnussen *et al.*, "Experimental study on the influence of controller firmware on multicopter actuator dynamics," in *Proc. IEEE Int. Symp. Robot. Sens. Environ.*, 2014, pp. 106–111.
- [11] W. Johnson, *Helicopter Theory*. Princeton, NJ, USA: Princeton Univ. Press, 1980.
- [12] M. Bangura *et al.*, "Aerodynamic power control for multirotor aerial vehicles," in *Proc. IEEE Int. Conf. Robot. Autom.*, 2014, pp. 529–536.
- [13] M. Bangura and R. Mahony, "Nonlinear dynamic modeling for high performance control of a quadrotor," in *Proc. Australas. Conf. Robot. Autom.*, 2012, pp. 1–10.
- [14] M. J. Stepaniak, F. V. Graas, and M. U. De Haag, "Design of an electric propulsion system for a quadrotor unmanned aerial vehicle," *J. Aircraft*, vol. 46, no. 3, pp. 1050–1058, 2009.
- [15] C. Ampatis and E. Papadopoulos, "Parametric design and optimization of multi-rotor aerial vehicles," in *Applications of Mathematics and Informatics in Science and Engineering*. New York, NY, USA: Springer, 2014, pp. 1–25.
- [16] B. A. Moffitt *et al.*, "Validation of vortex propeller theory for UAV design with uncertainty analysis," in *Proc. 46th AIAA Aerosp. Sci. Meeting Exhib.*, 2008, Art. no. 2008-406.
- [17] M. P. Merchant and L. S. Miller, "Propeller performance measurement for low Reynolds number UAV applications," in *Proc. 44th AIAA Aerosp. Sci. Meeting Exhib.*, 2006, Art. no. 1127:2006.
- [18] M. Cavcar, *The International Standard Atmosphere (ISA)*, vol. 30. Eskişehir, Turkey: Anadolu Univ., 2000.
- [19] E. Torenbeek and H. Wittenberg, *Flight Physics: Essentials of Aeronautical Disciplines and Technology, with Historical Notes*. Dordrecht, The Netherlands: Springer, 2009.
- [20] P.-Q. Liu, *Air Propeller Theory and Its Application* (in Chinese). Beijing, China: Beihang Univ. Press, 2006.
- [21] B.-L. Zhu, *Unmanned Aircraft Aerodynamics* (in Chinese). Beijing, China: Aviation Ind. Press, 2006.
- [22] C. Jun, S.-X. Yang, and M. Li, "Modeling and experimental analysis of UAV electric propulsion system," (in Chinese) *J. Aerosp. Power*, vol. 24, no. 6, pp. 1339–1344.
- [23] D. A. Lawrence and K. Mohseni, "Efficiency analysis for long-duration electric MAVs," in *Proc. Amer. Inst. Aeronaut. Astronaut. Infotech*, 2005, Art. no. 7090.
- [24] P. Lindahl, E. Moog, and S. R. Shaw, "Simulation, design, and validation of an UAVSOFC propulsion system," *IEEE Trans. Aerosp. Electron. Syst.*, vol. 48, no. 3, pp. 2582–2593, Jul. 2012.
- [25] RC Calculator on the Web, Feb. 27, 2016. [Online]. Available: <http://www.ecalc.ch/>
- [26] Flying Evaluation Website, Feb. 27, 2016. [Online]. Available: <http://www.flyeval.com/>
- [27] J. Yao *et al.*, "High-accuracy tracking control of hydraulic rotary actuators with modeling uncertainties," *IEEE/ASME Trans. Mechatronics*, vol. 19, no. 2, pp. 633–641, Apr. 2014.
- [28] W. Sun, H. Gao, and O. Kaynak, "Finite frequency H_∞ control for vehicle active suspension systems," *IEEE Trans. Control Syst. Technol.*, vol. 19, no. 2, pp. 416–422, Mar. 2011.
- [29] F. Hitchens, *Propeller Aerodynamics: The History, Aerodynamics & Operation of Aircraft Propellers*. Luton, U.K.: Andrews UK, 2015.
- [30] S. Chapman, *Electric Machinery Fundamentals*. New Delhi, India: Tata McGraw-Hill Education, 2005.
- [31] M. Orsag and S. Bogdan, *Influence of Forward and Descent Flight on Quadrotor Dynamics*. Rijeka, Croatia: InTech, 2012.



Dongjie Shi is working toward the M.S. degree at the School of Automation Science and Electrical Engineering, Beihang University (the Beijing University of Aeronautics and Astronautics), Beijing, China.

His main research interests include the multicopter design and altitude estimation.



Xunhua Dai received the B.S. and M.S. degrees in automation science and electrical engineering from Beihang University, Beijing, China, in 2013 and 2016, respectively, where he has been working toward the Ph.D. degree since 2016.

His main research interests include aerial refueling, flying control, and multicopter optimization design.



Xiaowei Zhang received the B.S. degree in automation science and electrical engineering from Beihang University, Beijing, China, in 2015. He is currently working toward the M.S. degree at the Shanghai Academy of Spaceflight Technology, Shanghai, China, since 2015.

His research interests include control science and engineering, modeling, and simulation.



Quan Quan received the B.S. and Ph.D. degrees in automation science and electrical engineering from Beihang University, Beijing, China, in 2004 and 2010, respectively.

He has been an Associate Professor with the School of Automation Science and Electrical Engineering, Beihang University, since 2013. His research interests include reliable flight control, vision-based navigation, repetitive learning control, and time-delay systems.